Interface structure and perpendicular exchange bias in $(Co/Pt)_n$/FeMn multilayers

Xiaosong Ji, Honglyoul Ju,[a] David E. McCready,[b] and Kannan M. Krishnan[c]
Department of Materials Science, University of Washington, Seattle, Washington 98195

(Received 4 January 2005; accepted 18 October 2005; published online 6 December 2005)

We have performed a critical experimental evaluation of the dependence of both perpendicular magnetic anisotropy and exchange bias on the structure of the ferromagnet (FM)/nonferromagnet and FM/antiferromagnet interfaces of $(Co/Pt)_n$ and $(Co/Pt)_n$/FeMn multilayers. The growth of these heterostructures by ion-beam sputtering was optimized and the characteristics of their interfaces were systematically controlled by varying the ion-beam energy from 250 to 1500 eV. Calculated effective anisotropy constants and exchange bias fields from hysteresis loops were correlated with both structural roughness and the degree of interdiffusion measured by x-ray reflectivity. Whilst the physical roughness remained unchanged, the degree of interdiffusion was found to increase with higher ion-beam energy—concurrently the magnetic anisotropy changed from perpendicular to in plane—leading directly to a decrease in exchange bias and coercivity.
 [DOI: 10.1063/1.2137878]

The phenomenon of exchange bias between a ferromagnet (FM) and an antiferromagnet (AFM), observed as a shift in the hysteresis loop when they are cooled through the blocking temperature, has attracted a lot of recent interest because of both intriguing physics and potential applications in information storage technologies.[1,2] In most cases, research on exchange bias has been carried out with in-plane magnetization, but recently, exchange bias with perpendicularly magnetized multilayers has also been investigated.[3–7] In spite of extensive research over the years, the microscopic origin of exchange bias is not fully understood; however, it is clear that exchange bias is an interfacial effect between a FM and AFM arising from a short-range FM-AFM exchange interaction at the interface. Thus exchange bias is very sensitive to the FM/AFM interface conditions. In addition, if the AFM is used to bias a $(Co/Pt)_n$ multilayer structure, where the enhanced perpendicular orbital magnetic moment (m_{orb}) of Co and Co_{3d}-Pt_{5d} interfacial hybridization gives rise to perpendicular anisotropy,[8] much work needs to be done to evaluate the complicated role played by both the FM/AFM and FM/NM interfaces in such perpendicular exchange biased multilayer systems. In this paper, we present a critical experimental evaluation of the dependence of both perpendicular magnetic anisotropy and exchange bias on the microstructure of the FM/NM (Co/Pt) and FM/AFM (Co/FeMn) interfaces, respectively. Heterostructures of $(Co/Pt)_n$ and $(Co/Pt)_n$/FeMn were grown by ion-beam sputtering with independent control of ion-beam energy and current.[9] In addition, this relatively lower-pressure processing results in less contamination compared with other methods (magnetron sputtering or thermal/electron-beam evaporation)[10] conventionally used for the growth of perpendicular exchange biased multilayers.

Initially, a variety of critical growth parameters for both the AFM layer and the FM multilayer stacks were carefully optimized. These parameters included the thicknesses of the individual Co (6 Å) and Pt (20 Å) layers, number of bilayers (5), and substrate temperature (room temperature). Subsequently, multilayers composed of $Pt_{200\ Å}/(Co_{6\ Å}/Pt_{20\ Å})_5/FeMn_{x\ Å}/Pt_{20\ Å}$ were grown on Si(001) substrates at room temperature. The chamber base pressure was 9×10^{-9} Torr and the Ar pressure during deposition was 1.2×10^{-4} Torr. An external magnetic field of 400 Oe, perpendicular to the thin-film plane, was applied during thin-film growth using a permanent magnet. A thick Pt buffer layer (200 Å) was deposited onto the Si substrate to introduce a Pt(111) growth orientation, the preferred orientation for perpendicular anisotropy of $(Co/Pt)_n$ (Ref. 11). The multilayers were also capped with a thin (~20 Å) Pt layer to prevent oxidization upon exposure to air. The magnetic properties were measured using a vibrating sample magnetometer (VSM). The samples were structurally characterized by θ-2θ x-ray diffraction (XRD) and XRR.

Figure 1 shows the room-temperature, out-of-plane hysteresis loops of three $(Co_{6\ Å}/Pt_{20\ Å})_5$ multilayer samples deposited at different ion-beam energies of 250, 500, and 750 eV. $(Co/Pt)_n$ multilayer grown at an ion-beam energy of 250 eV has the highest perpendicular anisotropy and a square hysteresis loop with almost 100% remnant magnetization (M_R). As the ion-beam energy increases, M_R decreased until $M_R/M_s \sim 10\%$ at an ion-beam energy of 750 eV. The effective anisotropy constant (K_{eff}) can be calculated from the energy difference between samples saturated along the in-plane and perpendicular directions,[7] using

[a]Also at the Department of Physics, Yonsei University, Seoul, Korea 120-749.
[b]Permanent address: Pacific Northwest National Laboratory, Richland, Washington 99352.
[c]Electronic mail: kannanmk@u.washington.edu

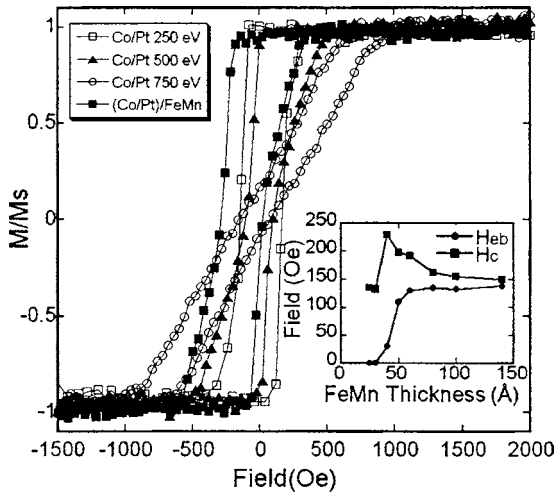

FIG. 1. Out-of-plane hysteresis loops of $(Co/Pt)_n$ multilayers grown at different Ar ion-beam energies (250, 500, and 750 eV) and biased $(Co/Pt)_n$/FeMn multilayers grown at an ion-beam energy of 250 eV. (Inset) Exchange bias field (H_{eb}) and coercivity (H_c) vs FeMn thickness.

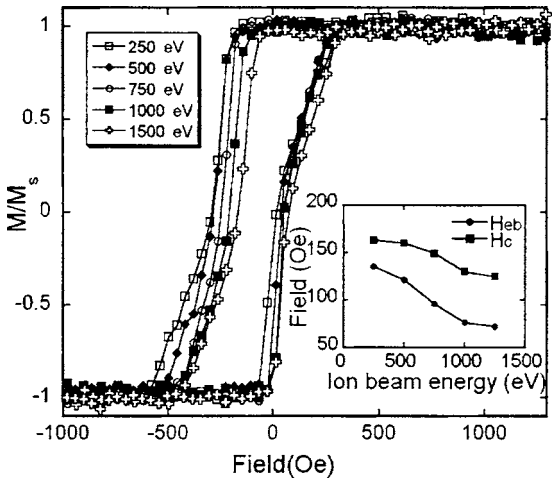

FIG. 2. Out-of-plane hysteresis loops of $(Co/Pt)_n$/FeMn multilayers with FeMn deposited at different Ar ion-beam energies. (Inset) Exchange bias field (H_{eb}) and coercivity (H_c) vs ion-beam energy.

$$K_{\text{eff}} = \frac{1}{V_{\text{FM}}} \int_0^{H_{\text{sat}}} (M_P - M_I) dH, \tag{1}$$

where V_{FM} is the total Co volume in the $(Co/Pt)_n$ multilayers, H_{sat} is the saturation magnetic field, and M_p, M_I are magnetizations along the perpendicular and in-plane directions. The calculated anisotropy constant for $(Co/Pt)_n$ is $K_{\text{eff}} = 4.17 \times 10^6$, 1.25×10^6, and -3.75×10^5 erg/cm^3 for multilayers grown at 250, 500, and 750 eV, respectively. From the decreasing magnitude and change in sign of K_{eff}, it is clear that the transition from perpendicular to in-plane anisotropy occurs with increasing ion-beam energy.

Figure 1 also shows a large shift in the hysteresis loop (H_{eb}) when a layer of FeMn was grown adjacent to the top Co layer (for the optimal ion-beam voltage of 250 eV). This H_{eb} for $(Co_{6\ Å}/Pt_{20\ Å})_5/FeMn_{x\ Å}$ is critically dependent (Fig. 1, inset) on the FeMn layer thickness (t_{AFM}). Below a critical thickness $t_{\text{AFM}} \sim 30$ Å, $H_{eb} \sim 0$. As t_{AFM} increases, H_{eb} also increases until it reaches a saturation value when $t_{\text{AFM}} \sim 60$ Å. Such dependence of H_{eb} on t_{AFM}, observed routinely in in-plane magnetized systems, has been attributed to the thermal stability of the AFM layer.[12] In addition, the coercivity (H_c) also reaches a peak value when $t_{\text{AFM}} \sim 40$ Å, due to the magnetization of FeMn being dragged by the $(Co/Pt)_n$ magnetization.[5]

It is clear that the lower ion-beam energy enhances the perpendicular anisotropy with the best results obtained for 250 eV. The ion-beam energy also affects the exchange bias field. Figure 2 shows the hysteresis loops of representative multilayers of $(Co_{6\ Å}/Pt_{20\ Å})_5/FeMn_{80\ Å}$. All the $(Co_{6\ Å}/Pt_{20\ Å})_5$ stacks were grown at an ion-beam energy of 250 eV, while the FeMn layers were grown at different ion-beam energies varying from 250 to 1500 eV. The ion-beam energy dependence of H_c and H_{eb} is shown in the inset of Fig. 2. It is noticed that H_{eb} drops rapidly from 135 to 45 Oe when the FeMn layers were grown at a higher ion-beam energy. H_c also decreased as the ion-beam energy increased, possibly due to the competition between perpendicular anisotropy induced by the Co/Pt interfaces and the large in-plane anisotropy induced at the terminating Co/FeMn interface together with the overall shape anisotropy of the film.

Figure 3 shows θ-2θ XRD scans from the same samples examined in Fig. 1. The diffraction data confirmed a preferred Pt(111) orientation in the stacks; Pt(200) was not observed. In addition to this Pt(111) peak, all four multilayers showed a satellite peak at 36.5°, which corresponds to a $(Co/Pt)_n$ superlattice bilayer period of 2.6 nm (Ref. 13). Sample (d) also shows a FeMn(111) peak at 42.5°, which is the favorable FeMn orientation for exchange bias.[14]

XRR measurements on the multilayers can be modeled for the density, thickness, and interface roughness.[15] Finite thickness oscillations with two different wavelengths are clearly distinguishable in Fig. 4; the short-wavelength oscillations correspond to the total thickness of the multilayers; while the longer-wavelength oscillations arise from the $(Co/Pt)_n$ superlattice of the film. A commercial software program REFS (Build 4.00.13, Bede PLC, England) was used to model the experimental XRR patterns to determine the critical thickness parameters (6 Å Co and 20 Å Pt), the number of bilayers ($n=5$) required for stabilizing perpendicular an-

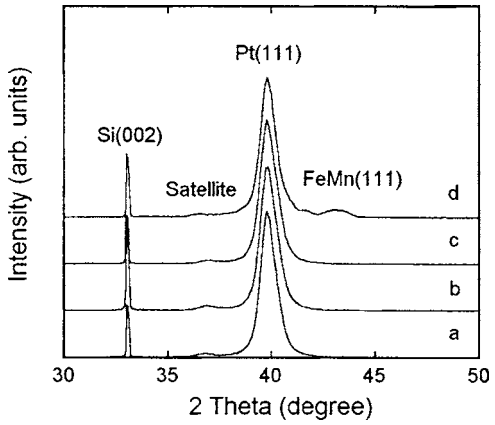

FIG. 3. $\theta-2\theta$ x-ray diffraction (XRD) of $(Co/Pt)_n$ multilayers grown at different Ar ion-beam energies: (a) 250, (b) 500, and (c) 750 eV. (d) $(Co/Pt)_n$/FeMn multilayer grown at an ion-beam energy of 250 eV.

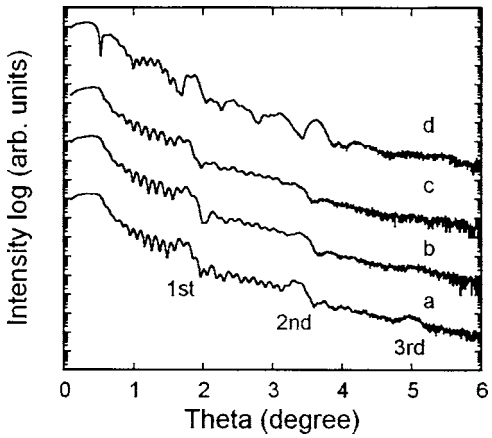

FIG. 4. X-ray reflectivity (XRR) of $(Co/Pt)_n$ multilayers grown at different Ar ion-beam energies: (a) 250, (b) 500, and (c) 750 eV. (d) $(Co/Pt)_n$/FeMn multilayers grown at an ion-beam energy of 250 eV.

isotropy, as well as the thicknesses of the Pt seed and FeMn layers. These data verify the excellent layered growth of these multilayers and indicate that ion-beam sputtering can grow high-quality multilayers even at room temperature. A comparison of the XRR measurements of multilayers grown at different ion-beam energies clearly shows that higher-energy deposition caused a more rapid falloff in satellite peak intensities. The third-order satellite reflection from the multilayer grown with 250 eV was well above background [Fig. 4(a)], but was not observed for the multilayer grown with 500 and 750 eV [Figs. 4(b) and 4(c)]. This indicates that either the interdiffusion (chemical effect) or interface roughness (structural) increases while ion-beam energy increases.

Further modeling of the XRR data makes it possible to differentiate the interdiffusion from interface roughness. The calculated roughnesses of the Co/Pt interfaces were ~2–4 Å and the Co/FeMn interface roughness was about 1.2 Å, which were both independent of the ion-beam energy. In contrast, the fits for the densities of the Co layers varied proportionally with ion-beam energy and, in all cases, were significantly higher than the bulk value (D_x=8.836 g/cm^3). The calculated Co layer density was ~150% of the bulk value for the sample grown at ion-beam energy of 250 eV, and increased to about 200% in samples grown at 750 eV. This result can be explained by considering that the energy of sputtered elements increases with increasing Ar ion energy and leads to a deeper penetration and larger interdiffusion. Based on the modeling of the XRR data we estimate that the interdiffusion of Pt atoms into the Co layer was about 20 at. % for an ion-beam energy of 250 eV, but substantially higher (45 at. %) when the ion-beam energy reached 750 eV.

Comparing these data with the hysteresis loops in Fig. 1, it is apparent that the degree of perpendicular anisotropy decreases as ion-beam energy and interdiffusion increase. Interdiffusion at the Co/FeMn interface also increase with ion-beam energy, leading to a decrease of the perpendicular exchange bias field (Fig. 2). It is believed that exchange bias will vanish as the penetration depth of FeMn reaches the thickness of the top Co layer.

XRR provides a measurement of the lattice parameters and disorder that is always averaged over the whole superlattice. Related data simulation uses the interface roughness often as a single parameter to investigate the interface disorder. However, in our $(Co/Pt)_n$/FeMn multilayer system, the calculated roughness in all cases is almost of the same magnitude as the Co layer thickness. To account for this, we use layer density as an independent parameter to study interdiffusion (short-range, chemical intermixing), and a "roughness" parameter for the long-range, physical/structural disorder, in fitting the XRR data. Fitting of XRR data to characterize roughness is indirect; however, quantitative interface structural characterization can be carried out by high spatial resolution energy-filtered transmission electron microscopy (EFTEM) in the cross-sectional geometry.[16] Such EFTEM makes it possible to directly probe the specific chemical distribution from individual layers, the lateral length scale, and the replication of disorder from layer to layer. This work is in progress.

In summary, high-quality $(Co/Pt)_n$/FeMn with perpendicular anisotropy and exchange bias has been grown by ion-beam sputtering. By varying ion-beam energy, the interdiffusion at the FM/NM and FM/AFM interfaces can be well controlled. Multilayers deposited at lower ion-beam energy have a lower chemical interdiffusion at the interface, and lead to a stronger perpendicular magnetic anisotropy and larger exchange bias.

This work was supported by the DoE Materials Science Division under Grant No. DE-FG03-02ER45987 and by the Campbell Endowment at UW. A portion of the research described in this paper was performed in the Environmental Molecular Sciences Laboratory, a national scientific user facility sponsored by the Department of Energy's Office of Biological and Environmental Research and located at Pacific Northwest National Laboratory.

[1] W. H. Meiklejohn and C. P. Bean, Phys. Rev. **102**, 1413 (1956).
[2] J. Nogues and I. K. Schuller, J. Magn. Magn. Mater. **192**, 203 (1999).
[3] B. Kagerer, Ch. Binek, and W. Kleemann, J. Magn. Magn. Mater. **217**, 139 (2000).
[4] S. Matt, K. Takano, S. S. P. Parkin, and E. E. Fullerton, Phys. Rev. Lett. **87**, 087202 (2001).
[5] F. Garcia, G. Casali, S. Auffret, B. Rodmacq, and B. Dieny, J. Appl. Phys. **91**, 6905 (2002).
[6] C. H. Marrows, Phys. Rev. B **68**, 012405 (2003).
[7] S. M. Zhou, L. Sun, P. C. Searson, and C. L. Chien, Phys. Rev. B **69**, 024408 (2004).
[8] N. Nakajima, T. Koide, T. Shidara, H. Miyauchi, H. Fukutani, A. Fujimori, K. Iio, T. Katayama, M. Nývlt, and Y. Suzuki, Phys. Rev. Lett. **81**, 5229 (1998).
[9] P. Blomqvist, K. M. Krishnan, and D. E. McCready, J. Appl. Phys. **95**, 8019 (2004).
[10] Ch. Binek, B. Kagerer, S. Kainz, and W. Kleemann J. Magn. Magn. Mater. **226**, 1814, (2001).
[11] C. H. Lee, R. F. C. Farrow, C. J. Lin, E. E. Marinero, and C. J. Lin, Phys. Rev. B **42**, 11384 (1990).
[12] K. Nishioka, S. S., Takao I., and S. Narishige, J. Appl. Phys. **83**, 3233 (1998).
[13] C. L. Canedy, X. W. Li, and G. Xiao, J. Appl. Phys. **81**, 5367 (1997).
[14] R. Jungblut, R. Coehoorn, M. T. Johnson, J. aan de Stegge, and A. Reinders, J. Appl. Phys. **75**, 6659 (1994).
[15] Z. H. Ming, A. Krol, Y. L. Soo, Y. H. Kao, J. S. Park, and K. L. Wang, Phys. Rev. B **47**, 16373 (1993).
[16] J. Santamaria, M. E. Gomez, J. L. Vicent, Kannan M. Krishnan, and I. Schuller, Phys. Rev. Lett. **89**, 190601 (2002).